J. Membrane Biol. 184, 171–183 (2001)
DOI: 10.1007/s00232-001-0086-1

The Journal of
Membrane
Biology

Permeabilization of Model Lipid Membranes by *Bacillus sphaericus* Mosquitocidal Binary Toxin and its Individual Components

J.-L. Schwartz[1,2], L. Potvin[1], F. Coux[2], J.-F. Charles[3], C. Berry[4], M.J. Humphreys[4], A.F. Jones[4], I. Bernhart[5], M. Dalla Serra[5], G. Menestrina[5]

[1]Biotechnology Research Institute, Montreal, Quebec, Canada, H4P 2R2
[2]Groupe de Recherche en Transport Membranaire, Université de Montréal, C.P. 6128, Succ. Centre-Ville Montreal, Quebec, Canada, H3C 3J7
[3]Institut Pasteur, Bactéries Entomopathogènes, 75724 Paris, France
[4]Cardiff School of Biosciences, Cardiff University, P.O. Box 911, Museum Avenue, Cardiff, CF10 3US, UK
[5]CNR-ITC, Centro di Fisica degli Stati Aggregati, Via Sommarive 18, I-38050 Povo, Italy

Received: 29 March 2001/Revised: 20 July 2001

Abstract. The high larvicidal effect of *Bacillus sphaericus* (*Bs*), a mosquito control agent, originates from the presence of a binary toxin (*Bs* Bin) composed of two proteins (BinA and BinB) that work together to lyse gut cells of susceptible larvae. We demonstrate for the first time that the binary toxin and its individual components permeabilize receptor-free large unilamellar phospholipid vesicles (LUVs) and planar lipid bilayers (PLBs) by a mechanism of pore formation. Calcein-release experiments showed that LUV permeabilization was optimally achieved at alkaline pH and in the presence of acidic lipids. BinA was more efficient than BinB, BinB facilitated the BinA effect, and their stoichiometric mixture was more effective than the full Bin toxin. In PLBs, BinA formed voltage-dependent channels of ≈100–200 pS with long open times and a high open probability. Larger channels (≥400 pS) were also observed. BinB, which inserted less easily, formed smaller channels (≤100 pS) with shorter mean open times. Channels observed after sequential addition of the two components, or formed by their 1:1 mixture (w/w), displayed BinA-like activity. *Bs* Bin toxin was less efficient at forming channels than the BinA/BinB mixture, with channels displaying the BinA channel behavior. Our data support the concept of BinA being principally responsible for pore formation in lipid membranes with BinB, the binding component of the toxin, playing a role in promoting channel activity.

Correspondence to: J.-L. Schwartz; e-mail: jean-louis.schwartz@bri.nrc.ca

Key words: *Bacillus sphaericus* — Pore-forming toxin — Planar lipid bilayers — Lipid vesicles — Calcein release — Ion channels

Introduction

Many strains of *Bacillus sphaericus* (*Bs*) are pathogenic to mosquito larvae. Pathogenicity results from the production of one or more protein toxins that act in the mosquito gut leading to the death of susceptible larvae. The most potent mosquitocidal strains of *Bs* owe their high toxicity to the presence of the binary toxin (Bin) composed of two proteins of 42 and 51 kDa (BinA and BinB respectively). These proteins are produced upon sporulation and are deposited as parasporal crystals within the exosporium [2]. For maximum toxicity, both components of the toxin need to be present in equimolar quantities [1, 19] although BinA alone is toxic to *Culex pipiens quinquefasciatus* cells in culture [1] and, when isolated from a recombinant *Bacillus thuringiensis* strain, BinA may also be toxic to mosquitoes [5, 23, 42].

The initial sequence of events that occurs when susceptible larvae of the mosquito *C. p. quinquefasciatus* ingest the binary toxin, has been elucidated. The BinB protein binds regionally to the gastric caecum and posterior midgut. BinA then appears to be directed to bind to the same regions of the gut by the presence of BinB (in the absence of BinB, BinA shows no specific binding) [44]. The interaction of the binary toxin with *C. p. pipiens* brush border membrane vesicles was shown to be mediated by a single class of receptor [51] identified as an alpha-glucosidase [52], which has recently been

cloned [15]. Receptor binding in *C. p. pipiens* was found to be entirely due to the BinB protein [11]. However, less is known of the mechanism of action of the binary toxin following these initial binding events.

Several studies have shown that the Bin toxins and their components profoundly affect the morphology and the ultrastructure of mosquito larval midgut epithelial cells [9, 16] and mosquito ovarian cell lines [21]. Of particular interest is the fact that Bin toxin internalization apparently was observed [18, 20, 44], suggesting that the protein may behave like other translocating bacterial toxins that are also pore formers [34, 35], like diphtheria toxin [25, 30], *Pseudomonas* exotoxin A [26, 39] and *Clostridium* neurotoxins [29]. Further indications that Bin toxin may induce membrane permeabilization were provided by an electrophysiological study conducted on a *C. p. quinquefasciatus* cell line, showing that whole-cell currents increased upon exposure to Bin or its individual components [13]. It was suggested that this overall reduced membrane resistance resulted from pore formation by the toxin, but it cannot be excluded that other mechanisms involving endogenous transport change may have also been responsible for the increased cell membrane permeability. So far, there is no direct evidence for membrane permeabilization by Bin toxins or their components. In this study, we show for the first time that the binary toxin and its individual components are capable of permeabilizing phospholipid vesicles under particular pH and lipid composition conditions. Furthermore, this membrane activity is most likely due to pore formation, as directly demonstrated in planar lipid bilayer experiments.

Materials and Methods

Chemicals and Solutions

Lipids used were egg phosphatidylcholine (PC), phosphatidylethanolamine (PE), phosphatidylserine (PS) and phosphatidic acid (PA) from Avanti Polar Lipids (Alabaster, AL), asolectin and cholesterol (chol) from Fluka (Buchs, Switzerland). Cholesterol used in PLB experiments was from Sigma (St. Louis, MO). All were at least 99% pure by TLC, according to the manufacturer. Calcein (M.W. 622.5), EDTA, and Sephadex-G50 were from Sigma-Aldrich (St. Louis, MO), Triton-X from Merck (Whitehouse Station, NJ). Prionex, a hydrolyzed porcine collagen of average mass 20 kDa, was purchased from Pentapharm (Basel, Switzerland). Tetracycline and trypsin were obtained from Serva (Heidelberg, Germany). For vesicle preparation and permeabilization experiments, the following solutions were used: solution A, which contained (in mM): 120 NaCl, 1 EDTA, 20 Tris-HCl, pH 7.5 and solution B made of (in mM) 100 NaCl, 1 EDTA with 20 HEPES-NaOH for pH 7.5 or 20 CAPS-NaOH for pH 9 to 11 (as indicated). For planar lipid bilayers (PLBs), the chamber solution contained (in mM) 150 KCl, 1 $CaCl_2$ and 10 Tris-HCl, pH 9.0.

Bs Toxin Preparation

The recombinant *B. thuringiensis* strain 4Q2-81 (pGSP10), expressing the *bin* operon from *Bs* strain 1593 was grown in a 20-l fermentor in UG liquid medium [22] containing 25 μg tetracycline per ml for 72 hours. Crystals were purified on a discontinuous sucrose gradient from a 25-times concentrated, washed and sonicated cell pellet [43]. Purified crystals were washed three times with sterile distilled water and stored at −20°C. Proteins were solubilized in 50 mM NaOH, neutralized and dialyzed in 20 mM sodium phosphate buffer pH 8. Protoxin was activated to toxin by addition of bovine pancreatic trypsin (0.52 U/mg with a protein to trypsin ratio 100:1 w/w) for 2 hr at 37°C. Samples were concentrated by ultrafiltration on Centricon 30 (Millipore-Amicon, Bedford, MA) and protein concentration was determined by the method of Bradford [3] using the Bio-Rad protein-assay dye reagent and bovine serum albumin as a standard (both from Bio-Rad, Cambridge, MA). Individual recombinant *Bs* BinA and BinB toxin proteins were expressed in *Escherichia coli* and purified as fusions with glutathione-S-transferase as described previously [44].

Permeabilization of Unilamellar Lipid Vesicles

Large unilamellar vesicles (LUVs), loaded with calcein, were prepared by the extrusion technique [37]. The ratios reported for lipid mixtures were calculated on a molar basis. Multilamellar liposomes (typically at a total lipid concentration of 4 mg/ml) were suspended in a solution containing 80 mM calcein (neutralized with NaOH), and subjected to 6 cycles of freezing and thawing. They were then repeatedly passed through two stacked polycarbonate filters (Osmonics, Livermore, CA) of 100-nm pore size, using a two-syringe extruder (LiposoFast Basic unit, Avestin, Ottawa, Canada) as previously described [54]. The untrapped dye was removed by spin-washing through Sephadex G-50 minicolumns (Pierce, Rockford, IL), equilibrated with vesicle solution. The permeabilizing activity of toxins at doses between 3.1 and 200 μg/ml, i.e., 54 nM–2.16 μM of non-activated Bin toxin, 73.8 nM–4.76 μM of BinA or 60.8 nM–3.92 μM of BinB proteins, was evaluated by measuring the release of calcein [32, 39]. Single kinetic experiments were performed using a photon-counting spectrofluorimeter (Fluoromax, JY Horiba, Edison, NJ). Aliquots of washed LUVs were placed in a 1-cm light-path stirred quartz cuvette, in a total volume of 1.0 ml of solution A. The final lipid concentration was between 1 and 2 μg/ml. After adding the toxins, the time-course of calcein release was recorded as an increase in the fluorescence emitted at 515 nm with the excitation set at 493 nm (both slits were set at 5 nm). Such fluorescence signal results from the dequenching of the dye when it is released from the LUVs and diluted in the external medium. Screening experiments were performed similarly, but using a fluorescence microplate reader (Fluostar, SLT, Austria). In this case, samples were excited at 485 nm and the emitted fluorescence was continuously measured at 538 nm. A 96-well microtiter plate was filled with 200 μl of vesicle solution (A or B) and the desired amount of toxin and vesicles. The final lipid concentration was between 2 and 5 μg/ml. To avoid unspecific interactions of the vesicles and the toxins with the plastic walls of the plate, it was preconditioned by incubation for 1 hr with vesicle solution containing 0.1 mg/ml Prionex. This stabilizing solution was eventually removed. In all cases, the experiments were conducted at room temperature and the time course of the percentage of toxin-induced release was calculated by:

$$R\%(t) = 100(F(t) - F_i)/(F_m - F_i), \quad (1)$$

where F_i is the initial fluorescence before adding the toxins, $F(t)$ the value at time t, and F_m the maximal value after addition of 1 mM Triton X-100. Spontaneous release of calcein was usually quite negligible

(less than 3%); if present, it was subtracted from the toxin-induced release.

Pore Formation in Planar Lipid Bilayers

PLBs [41] were formed from a 7:2:1 (w/w) lipid mixture (25 mg/ml final concentration in decane) of PE, PC and chol. The bilayer was painted, using disposable glass rods made from prepulled, sealed-tip Pasteur pipettes, across a 250-μm orifice separating two small volume chambers (5 ml *trans*, 3 ml *cis*) and pretreated with the above lipid mixture dissolved in chloroform. Membrane thinning was monitored by visual observation through a binocular dissection microscope and was assayed electrically. Typical membrane capacitance values ranged between 150 and 200 pF. Under the conditions used in this study, membranes remained stable for hours. At the beginning of each experimental session, they were tested for 15–20 min, at various holding voltages, for the absence of channel-like activity. Protein incorporation was promoted by stirring the solution in the *cis* chamber using a magnetic stir bar and by applying holding voltages between ±100 mV. Channel activity was monitored by step changes in the current recorded during holding test voltages applied to the planar lipid bilayer. All experiments were performed at room temperature (20–22°C) in PLB solution.

Standard incorporation protocols were used for the *Bs* Bin toxin or its individual BinA and BinB components [46], i.e., 15-μg aliquots of the proteins were added to the *cis* chamber after bilayer formation to reach final concentrations of 5 μg/ml of *Bs* toxin, i.e., 54 nM of non-activated Bin toxin, 119 nM of BinA or 98 nM of BinB proteins. In experiments designed to investigate the interaction between the individual BinA and BinB components of the Bin toxin, the following protocol was used: after addition to the *cis* chamber of a 15-μg aliquot of the first component to be tested, channel activity was initially recorded for 30 min. A 15-μg aliquot of the second component was then injected in the same chamber and recording was resumed for another 30-min period. The phospholipid bilayer was then broken by a light mechanical tap to the setup and repainted immediately thereafter for incorporation into the lipid bilayer of the 1:1 (w/w) mixture of the two toxin components, a procedure equivalent to starting a new experiment with the 1:1 (w/w) mixture of the two components. Recording was then performed for an additional 30 min. This protocol is schematically illustrated in the insert of Fig. 8.

Electrical connections between the chambers and the recording instrumentation were made with Ag/AgCl electrodes and agar salt bridges (2% in 0.2 M KCl, 1 mM EDTA). Single-channel currents were recorded with an Axopatch-1D patch-clamp amplifier (Axon Instruments, Foster City, California), filtered at 5 kHz, displayed on an oscilloscope (Kikusui 5020A, Tokyo, Japan), pulse-code modulated (CRC VR-100A, Instrutech, Great Neck, New York) and stored on videotape. Currents were played back, filtered at 600 Hz through an analog 8-pole Bessel filter (Model 902, Frequency Devices, Haverhill, Massachusetts) and digitized at a 2.5-kHz sampling frequency using a Labmaster TL-125 (Axon Instruments) and Axotape version 1.2.01 software (Axon Instruments). Analysis was performed on a personal computer using pClamp version 5.5.1 software (Axon Instruments).

For each applied voltage, current amplitudes were measured on the recorded traces. For some voltages, current amplitude histograms were generated. Channel conductances were estimated from the slopes of the linear regressions on the data points from the current-voltage relations. Due to the multichannel nature of most records, no attempt was made to determine the kinetic properties of the *B. sphaericus* channels, as multichannel activity rendered the interpretation of open-time and closed-time analyses rather complicated [38]. However, whenever possible, the estimated mean probability of N channels being open (NP_o) was calculated as t_o, the sum of the total open times spent by N observable channels at each open state level, over t_i, the total recording time interval.

Applied voltages are defined with respect to the *trans* chamber, which was held at virtual ground. Positive currents (i.e., currents flowing through the planar lipid bilayer from the *cis* chamber to the *trans* chamber) are shown as upward deflections. The direction of current flow corresponds to positive charge movement.

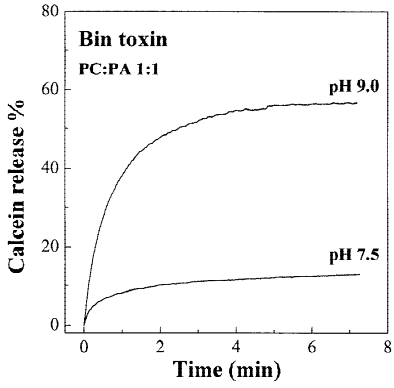

Fig. 1. Calcein release from lipid vesicles exposed to the full, non-activated *Bs* Bin toxin. At time zero, 200 μg/ml of toxin was added to a 1-cm stirred quartz cuvette containing around 2 μg/ml of washed LUVs in a total volume of 1 ml of solution B. The pH was adjusted to either 7.5 or 9.0, as indicated. LUVs were made of PC:PA (molar ratio 1:1). Calcein fluorescence was determined with a spectrofluorimeter (at 493-nm excitation and 515-nm emission wavelengths).

Abbreviations

Bs, *Bacillus sphaericus*; LUV, large unilamellar vesicle; PLB, planar lipid bilayer; PC, phosphatidylcholine; PE, phosphatidylethanolamine; PS, phosphatidylserine; PA, phosphatidic acid; PI, phosphatidylinositol; chol, cholesterol; Bin, wild-type, non-activated binary toxin; BinA, non-activated toxin 42 kDa component; BinB, non-activated toxin 51 kDa component.

Results

Permeabilization of Large Unilamellar Vesicles by *Bs* Bin Toxins

Effects of Bs *Bin Toxin*

To study the effects of *Bs* Bin toxin on lipid vesicles we performed fluorimetric calcein-release experiments. Under suitable conditions, a fluorescence increase was observed after exposing the vesicles to *Bs* Bin toxin, indicating that calcein leaked out (Fig. 1). Using vesicles composed of PC:PA (molar ratio 1:1) the observed leakage was higher at pH 9 than at pH 7.5.

A fluorescence microplate reader was used to screen the conditions for optimum release. First we tested the

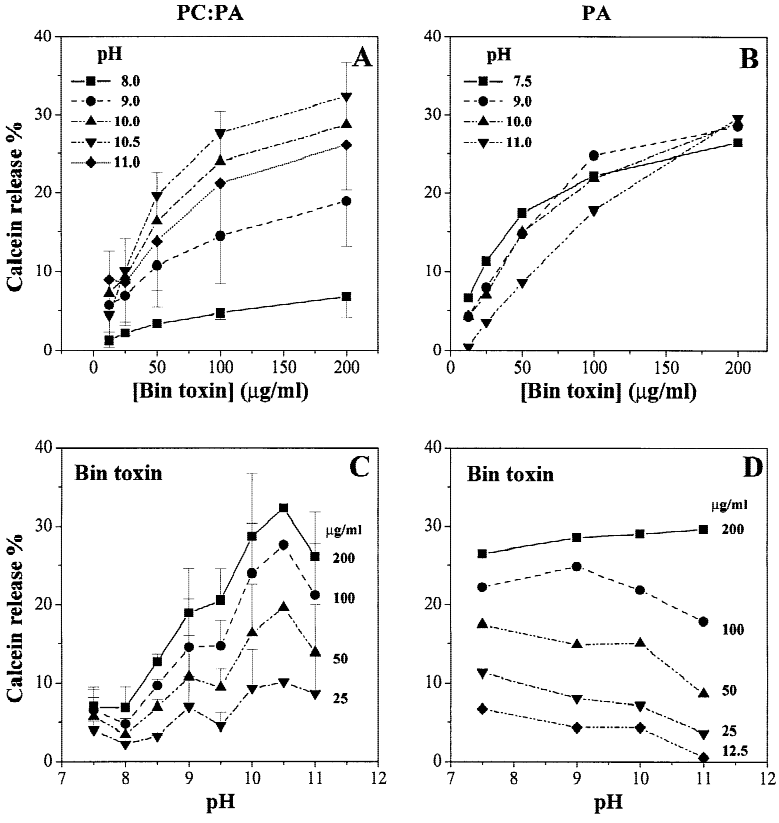

Fig. 2. Effects of pH and toxin concentration on the permeabilizing activity of the full Bin toxin on LUVs. Panels *A* and *B*: Concentration dependence of the steady-state calcein release at different values of pH and with LUVs made of either PC:PA (1:1) or pure PA (panel *A* and panel *B*, respectively). Panels *C* and *D*: pH Dependence of the same parameter at different toxin concentrations and with the same two lipid compositions. The experiments with PC:PA vesicles were done in triplicate (data are means ± SEM), whereas those with pure PA were single determinations. All experiments were performed with a fluorescence microplate reader (at 485-nm excitation and 538-nm emission wavelengths) using 5 μg/ml of lipid vesicles in solution A whose pH was adjusted by addition of concentrated NaOH. Other conditions were the same as in Fig. 1.

effects of the lipid composition at pH 9 and 10. The following lipid compositions were compared: asolectin, PE:PC:chol (7:2:1 molar), PE:PC:chol:PS (7:2:1:2.5), PC:PA (1:1) and pure PA. At both pH, release was observed only in the presence of PA, whereas asolectin, PE:PC:chol:PS and PE:PC:chol vesicles were all refractory. Considering that PC, PE and chol are neutral lipids in this pH range, whereas PA and PS are negatively charged and asolectin is a phospholipid mixture containing around 25% of negatively charged molecules, mainly PS [31], it follows that a suitable amount of negatively charged lipids is required for an efficient interaction.

The effects of pH and toxin concentration (in the range 12.5 to 200 μg/ml) with the two sensitive lipid compositions (PC:PA = 1:1 and pure PA) are reported in Fig. 2. Panels *A* and *B* show the concentration dependence at different values of pH, whereas panels *C* and *D* show the pH dependence at different concentrations. The experiments, conducted in triplicate, showed a pH dependence with an optimum activity around pH 9–10 (more pronounced in the case of PC:PA vesicles) and a nonlinear dose-dependence indicating saturation at higher doses. Up to the highest concentration tried (200 μg/ml), the trypsin-activated form was less active than the non-activated one at any pH and with any lipid composition (*not shown*), indicating that the proteolytic step is not necessary for interaction with purely lipidic membranes.

Effects of the Individually Expressed Bin Components

The effects of BinA and BinB, either alone or added separately at different times and molar ratios, are summarized in Fig. 3. Panel *A* shows the effect of BinA alone or in combinations with BinB (at the reported molar ratios). In these experiments the vesicles were first exposed to one component for almost 1 hr, then the second component was added for another hour. We reported the release in stationary conditions at the end of the experiment. For comparison, the result of having both components since the beginning is also shown. It appeared that BinA was able to permeabilize the vesicles by itself, but that large concentrations and longer exposures were needed. Interestingly, BinB improved the effect of BinA, although, in the steady state, neither the amount of BinB nor the order of addition changed the final release (but it affected its rate, *see* panel *C*). Panel *B* shows the effect of BinB either alone or in combination with different molar ratios of BinA. In this case clear differences were observed, suggesting that BinB alone could not permeabilize the vesicles to a substantial extent, but again that it improved the effect of BinA. Under these conditions, the amount of BinB required to

reach a given R% (*see* Eq. 1) was the lower the larger the amount of BinA present. When the effect of the pair (50 μg/ml of each component), with the three different protocols of addition (either together, or either one of the two components first) was compared, it appeared that the best strengthening effect of BinB, at least in terms of rate, was observed when it was already present at the moment of addition of BinA (*see* panel *C*). If BinA was added long before BinB, there was little, if any, strengthening effect.

Effects of the Mixture of Individually-expressed Components

The effects of the two components BinA and BinB, separately expressed in *E. coli* and individually purified, was studied next. The same amounts of the two components were added together to compare the reconstituted pair with the non-activated Bin toxin. The effect of the proteins on PC:PA (1:1) vesicles at different pH and toxin concentration was measured with the fluorescence microplate reader and is summarized in Fig. 4. The time course of calcein release produced by different toxin concentrations is shown in panel *A* of Fig. 4. Release was observed at concentrations ≥25 μg/ml of each component, slightly less than what was observed with the Bin mixture. The dose dependence of permeabilization at different pH is shown in panel *B*. The sigmoidal shape of these curves suggests a cooperative effect, more marked than that of the Bin mixture. Finally, the pH dependence is shown in panel *C* of Fig. 4. At 25 μg/ml

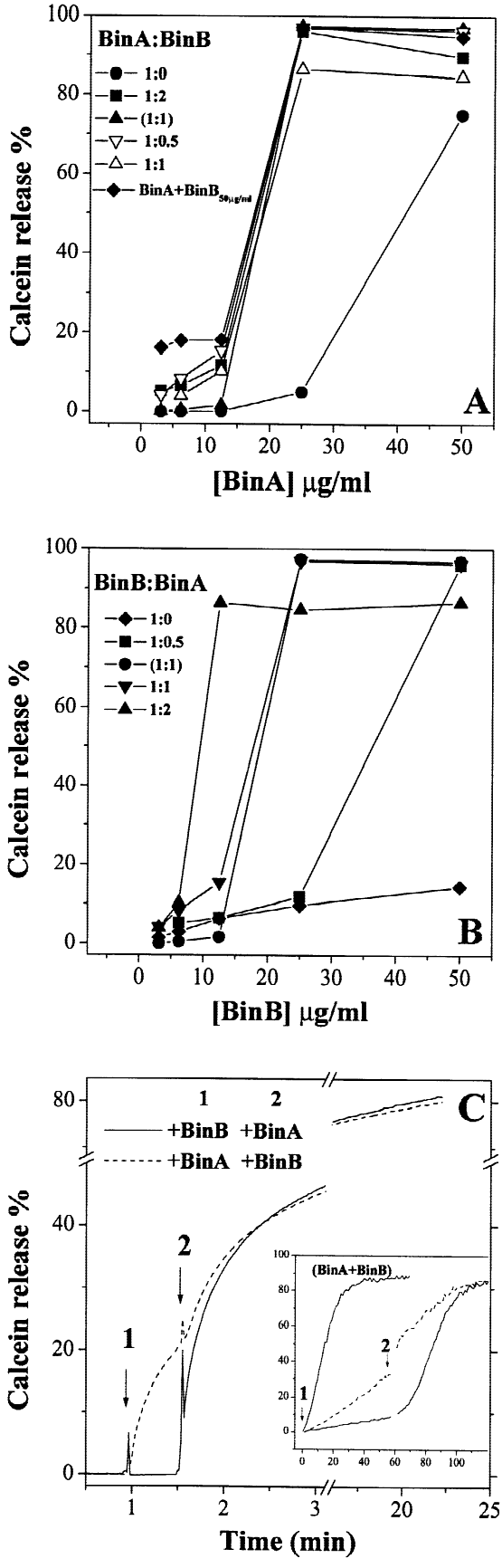

Fig. 3. Permeabilizing activity of recombinant BinA and BinB toxins. Calcein release was determined as in Fig. 2 except that BinA and BinB, separately expressed in *E. coli* and individually purified, were either used alone or added separately at different times and molar ratios. LUVs were made of PC:PA (1:1). Data points in panel A and B correspond to the steady-state calcein release. Panel *A*: Effect of BinA alone or in combination with different molar ratios of BinB (as indicated in the panel legend) at pH 8.0. The vesicles were first exposed to one component (first number of the molar ratio in the panel legend) for 1 hr, then the second component was added for another hour (second number of the molar ratio in the panel legend). Data with both components added together at the beginning of the experiment are shown for comparison (molar ratio given in parentheses in the panel legend). Data of an experiment in which the concentration of BinA was variable and that of BinB (added at the second step) was constant and always in excess (50 μg/ml) is also represented (filled diamonds). Panel *B*: Effect of BinB alone or in combination with BinA at various molar ratios. The sequence of component addition is described the same way as in panel A. Panel *C*: Time course of the effect of BinA and BinB added in inverse order as observed in the fluorimeter at pH 9.0 (34 μg/ml BinA and 20 μg/ml BinB). The insert shows the results of the same experiments performed in the microplate reader, with all three possible protocols of addition, i.e., together (trace labeled '(BinA+BinB')), or either one component first. In this particular case the concentration of each component was 50 μg/ml and pH was 8.0.

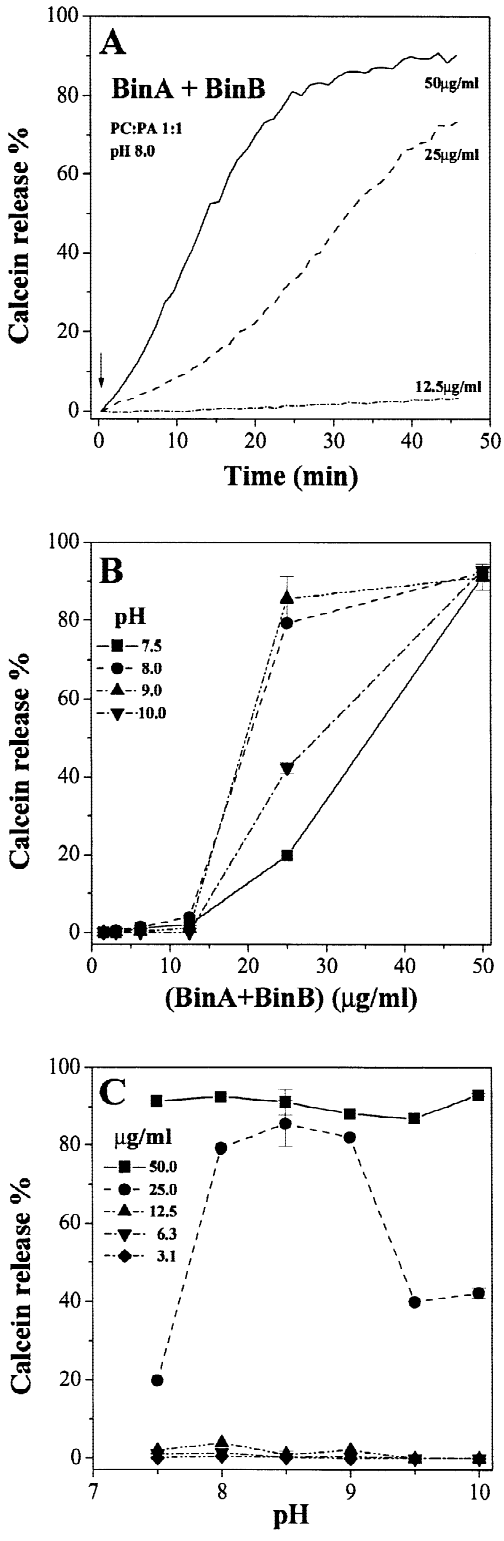

Fig. 4. Permeabilization of LUVs by recombinant BinA and BinB added at the same time and at the same w/w ratio. Experimental conditions are as in Fig. 3. Panel *A*: Time course of calcein release resulting from LUV exposure to different concentrations of toxin (as indicated) at pH 8.0. Panel *B*: Dose dependence of the permeabilization effect for different pH values. Panel *C*: pH Dependence of permeabilization at different toxin doses.

there was a clear optimum of vesicle permeabilization between pH 8 and 9, whereas at 50 μg/ml the effect was very high and independent of pH.

Ion Channels Formed by *Bs* Toxins in Planar Lipid Bilayers

Effects of Bs *Bin Toxin*

The ability of the *Bs* Bin toxin to form functional channels was tested in artificial phospholipid membranes. A first set of experiments was conducted on native Bin toxin ($n = 5$). Under our experimental conditions, the non-activated toxin displayed channel activity in one experiment. Membrane incorporation appeared to be unstable, with poorly resolved current steps (Fig. 5, upper left panel) and the channels displayed rapid flickering and short lived events. Their estimated conductance was between 20 and 300 pS (Fig. 5, lower left panel). The channels appeared to be voltage-dependent with a mean NP_o of about 50% at +60 mV and almost 100% at −60 mV. The trypsin-activated Bin toxin also formed channels in one experiment (out of 3). Toxin incorporation was more stable and the channels were better resolved than those displayed by the non-activated toxin (Fig. 5, upper right panel). Channel conductances ranged between 25 and 250 pS (Fig. 5, lower right panel), but most current steps corresponded to conductances of 70–130 pS. An estimate of the mean NP_o of the channels indicated that the trypsinized toxin was more active at negative voltages ($NP_o = 65\%$ at −60 mV vs. 24% at +60 mV).

Effects of Individually-expressed Bin Components and their 1:1 (w/w) Mixture

In the next set of experiments, the non-activated components of the Bin toxin were individually tested for channel formation. With BinA, well-resolved channels were observed in 9 experiments (out of a total of 11). In several experiments, at least one channel remained open almost all the time and several current steps lasting for more than 50–100 msec could be observed relative to this background activity. A typical record is shown in Fig. 6 (left panel, upper trace). In this particular experiment, three distinct current levels were present at +40 mV: the conductance of the background channel, which remained open for most of the experiment, was close to 170 pS and at least two other channels of about the same size were active. A different kinetic behavior was observed in a few experiments (Fig. 6, left panel, middle and lower traces). For positive voltages, the currents seemed either to remain in a rather noisy, long-lasting open state or to flicker rapidly between the closed state

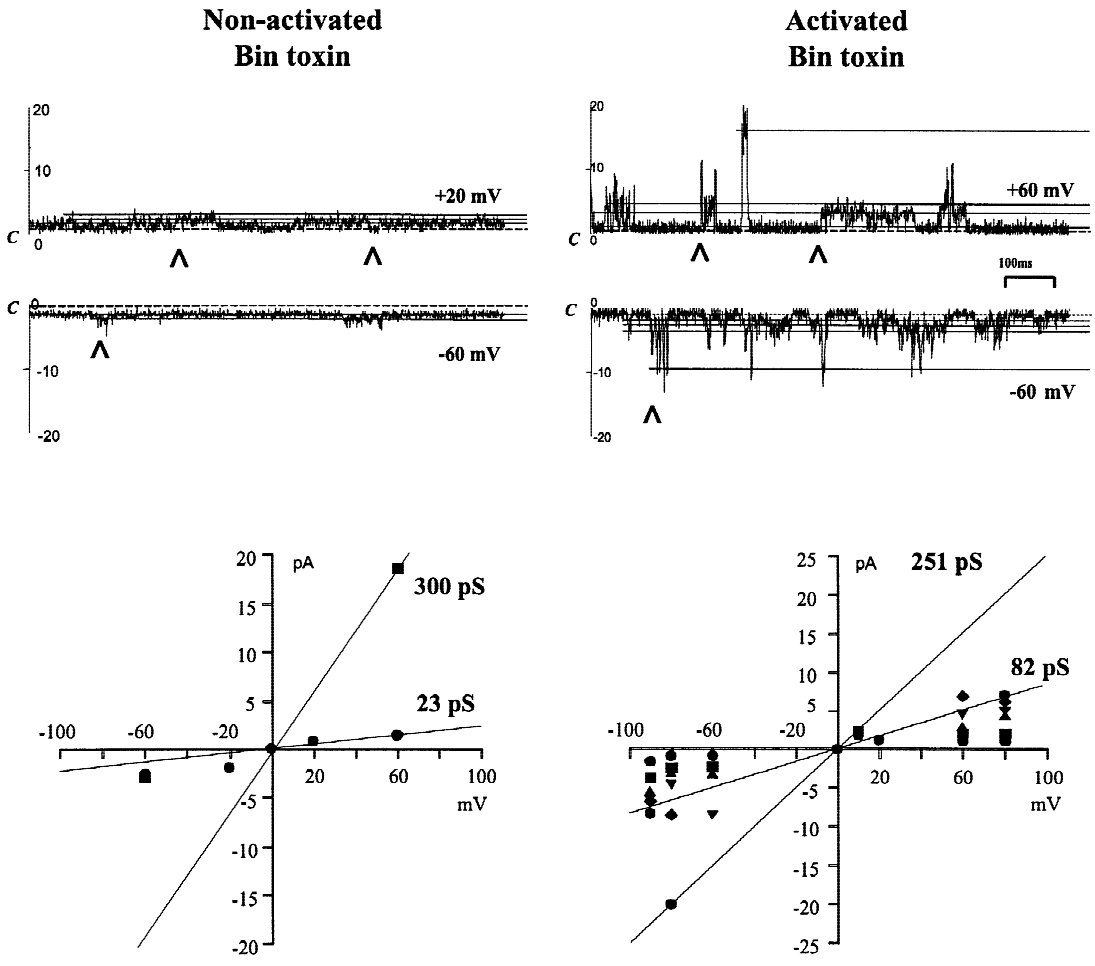

Fig. 5. Single-channel currents observed after addition of the full Bin toxin to the *cis* side of the planar lipid bilayer to a 5-μg/ml final protein concentration and representative current-voltage relations of the channels formed by the full toxin. *Upper panels*: Vertical axes are currents (in pA). Examples of fairly well-resolved transitions from one current level to another are indicated by vertical caret signs under the traces. Horizontal lines were drawn to show some of the conductance levels. Dotted lines, with the letter *C* at their left, indicate the estimated closed states of the channels. Applied voltages are given near the traces. *Upper left panel*: Non-activated Bin toxin. At least three channels were active in this experiment. The most active had a main conductance of approximately 40 pS. A larger, 300-pS channel was also occasionally observed (*not shown*). *Upper right panel*: Trypsin-activated Bin toxin. Several channels were observed with conductances ranging from 25 to 250 pS. Channel activity was higher and current steps were better resolved in the case of the activated *Bs* Bin toxin. *Left lower panel*: Current-voltage relations of the non-activated Bin toxin. *Right lower panel*: Current-voltage relations of the activated Bin toxin. For each holding voltage, data points represent single-channel currents corresponding either to transitions between successive opening levels or, when the closed state could be unambiguously identified, to transitions from the closed state to the first open-state level. Data from the same experiment are shown with identical symbols. Note that far more data could be extracted from experiments on the activated Bin toxin. Channel conductances for a few representative experiments were calculated as the slope of the straight lines obtained by visual fit (when three or fewer data points were available in an experiment) or linear regressions to the data points.

and a different open state at a higher conductance level. For negative voltages, a large background channel (approx. 225 pS) remained always open and at least one second channel displaying short-lived events, was active. Overall, the conductances of BinA, as determined from current measurements made relative to the background channel current level, ranged between 20 and 700 pS, occasionally with a few very large channels exceeding 900 pS. A larger variety of conductance levels was observed for positive voltages (Fig. 6, lower left panel), suggesting a voltage-dependent conductance. However, the channels made by the BinA protein were not voltage-dependent, i.e., their level of activity did not seem to vary with voltage: the mean NP_o of the channels was found to be around 45–50% at both +40 and −40 mV.

The larger component of the binary toxin, BinB, also formed channels in planar lipid bilayers under our experimental conditions in 5 experiments (out of a total of 10). In most experiments, the current traces resembled those observed with the non-activated full toxin: the appearance was hairy and the channels were small and poorly resolved (Fig. 6, right panel, upper and middle

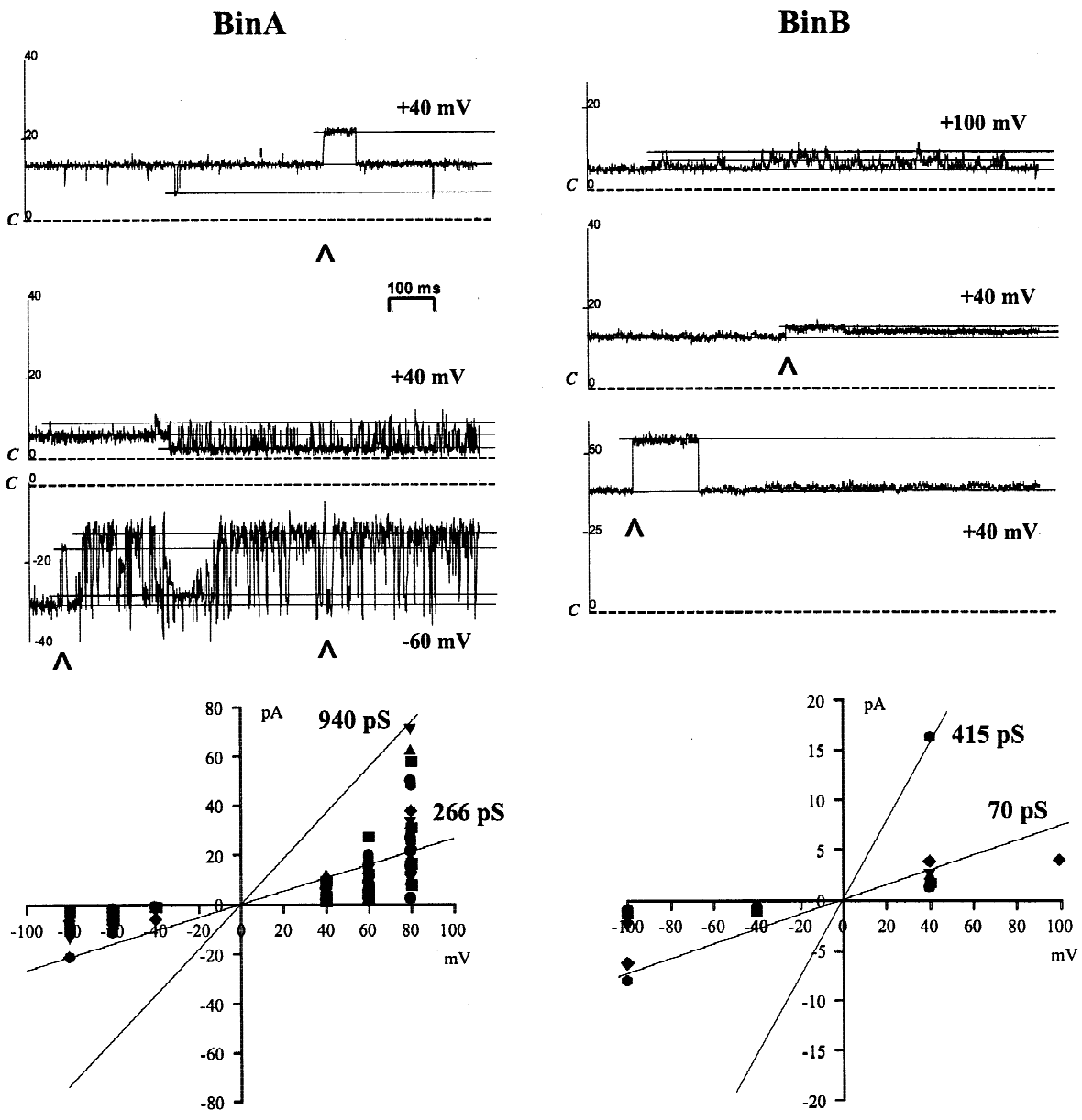

Fig. 6. Channel activity of the individual components of the Bin toxin and representative current-voltage relations of the channels formed by the full toxin. Single-channel currents observed after addition to the *cis* side of the bilayer of BinA to a final concentration of 5 μg/ml or BinB to a final concentration of 5 μg/ml. Vertical axes are currents (in pA). Examples of well-resolved transitions from one current level to another are indicated by vertical caret signs under the traces. Horizontal lines show the various conductance levels. Dotted lines, with the letter *C* at their left, indicate the estimated closed states of the channels. Applied voltages are given near the traces. *Upper left panel*: Channels formed by BinA, the 42-kDa component of the Bin toxin. At +40 mV (upper trace), three 170-pS channels were observed, two of them remaining open most of the time. At the same voltage, in another experiment, channel activity assumed a different pattern with current flickering between two subconductance levels. At −60 mV, a large channel was observed (266 pS) with both long openings and extremely short-lived fluctuations from a constantly open state at −13.5 pA. Representative records of 9 successful experiments. *Upper right panel*: Channels formed by BinB, the 51-kDa component of the bin toxin. The two upper traces show typical activity of BinB channels, with conductances of approximately 40 and 100 pS, and no evidence of full closure of all the channels. The lower trace illustrates a different type of channel. In this experiment, the current was continuously flowing through one or more large channels that never closed, and a well-resolved 415-pS channel could be observed. Representative records of 5 successful experiments. *Left lower panel*: Current-voltage relations of BinA. *Right lower panel*: Current-voltage relations of BinB toxin. For each holding voltage, data points represent single-channel currents corresponding either to transitions between successive opening levels or, when the closed state could be unambiguously identified, to transitions from the closed state to the first open-state level. Data from the same experiment are shown with identical symbols. Note that far more data could be extracted from experiments on BinA than BinB. Channel conductances for a few representative experiments were calculated as the slope of the straight lines obtained by visual fit (when three or fewer data points were available in an experiment) or linear regressions to the data points.

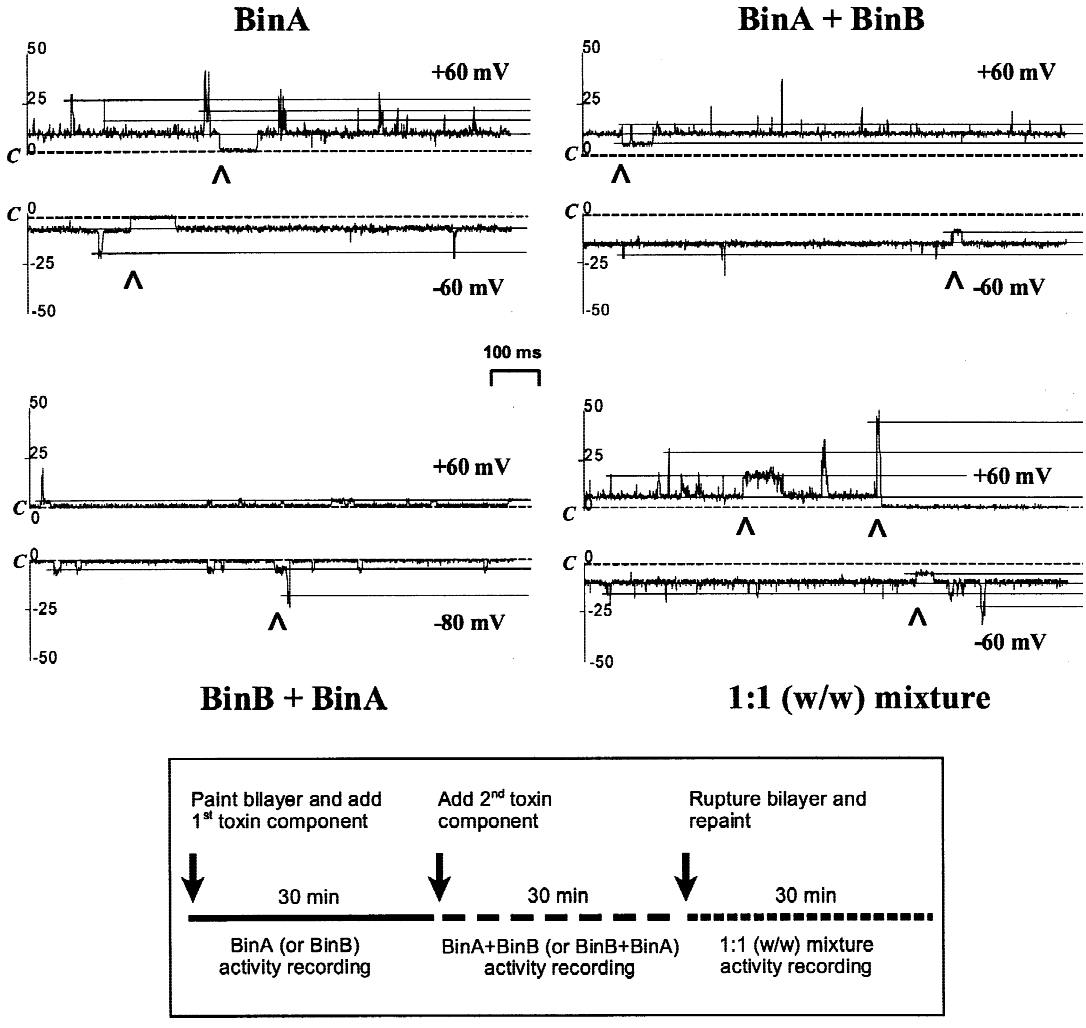

Fig. 7. Single-channel currents observed after sequential addition of the Bin toxin components to the *cis* chamber to a final concentration of 5 μg/ml, and their 1:1 (w/w) mixture. The titles *BinA+BinB* above the upper right panel and *BinB+BinA* below the lower left panel refer to the addition of BinA followed by that of BinB, or the addition of BinB followed by that of BinA, respectively, as illustrated in the insert given at the bottom of the figure, which describes the experimental protocol used in these experiments. Vertical axes are currents (in pA). Examples of well-resolved transitions from one current level to another are indicated by vertical caret signs under the traces. Horizontal lines show the various conductance levels. Dotted lines, with the letter *C* at their left, indicate the closed states of the channels. Applied voltages are given near the traces. Representative records of 9 (upper left panel), three (upper right panel), two (lower left panel) and 9 successful experiments (lower right panel).

traces). In most experiments, large background currents were observed, corresponding to conductances of at least 330 pS. These currents could be due either to BinB pores that remained locked in the open state or to leakage through the bilayer phospholipid arrangement being disrupted by the BinB protein. In one experiment, well-defined current steps of large amplitude were recorded, corresponding to a 400 pS conductance channel (Fig. 6, right panel, lower trace). The most common conductances were in the 40 to 100 pS range, but higher levels (up to 415 pS) were sometimes recorded (Fig. 6, lower right panel). The estimated NP_o of the channels was 90% at −40 mV and 70% at +40 mV, suggesting a slight voltage-dependence of the BinB channels.

The effect of sequential addition of the two individual components of the binary toxin was investigated (Fig. 7). Following a 30-min recording period of BinA channel activity, the same amount of BinB was added to the *cis* chamber using the protocol described in the insert of Fig. 7. In 3 experiments (out of a total of 6), the channels remained active and displayed the same behavior as BinA alone (Fig. 7, upper right panel), as previously described. On the other hand, when the BinA components was added after BinB channels had been active for 30 min, channel activity was only maintained in 2 experiments (out of 6) and the remaining channels adopted the behavior observed with the BinA protein alone (Fig. 7, lower left panel).

Channel formation by the mixture of BinA and BinB proteins was investigated as the last step of the sequential-addition experiments described above, following phospholipid membrane rupture and restoration in the presence of equal amounts of the two individual components in the *cis* chamber (*see* protocol in insert of Fig. 7). In all of the 9 experiments BinA-like channels were observed (Fig. 7, lower right panel).

Discussion

The permeabilizing ability of the *Bs* Bin toxin was investigated using large unilamellar vesicles and planar lipid bilayers. Our results strongly indicate that these proteins act as pore-forming toxins in a mode of action that appears to be similar to that of *B. thuringiensis* (*Bt*) toxins [24, 27, 33, 36, 45, 46, 47, 53] and other bacterial toxins [28, 40]. In susceptible insect gut cells, like *Bt* toxins, *Bs* Bin toxin may thus increase the permeability of the plasma membrane of mosquito epithelial cells and cause the observed cell swelling and finally larval death.

Vesicle permeabilization was demonstrated here by the passage of calcein through LUV membranes. Hydrated Stokes radius of calcein can be estimated to 0.75 nm [55], which suggests that the pores formed by the toxin in the vesicles were at least 1.5 nm in diameter. Clear permeabilization was attained in an alkaline pH environment, with a maximum between pH 9 and 10 depending on experimental conditions. The observed reduction of activity when the pH exceeded 10.5 might be due to a different conformation of the toxin at this pH, to the double ionization of the PA molecule, which occurs with a *pK* 9.5 [8], or both. The finding that activity is optimum near pH 10 is relevant, because the environment in which the toxin becomes effective, i.e., the gut of mosquitoes, is indeed alkaline (between pH 10 and 11 [14]). A similar pH dependence was also observed with several *Bt* toxins in planar lipid bilayers and brush border membrane vesicles [24, 27, 33, 36, 46, 53]. On the other hand, liposome permeabilization by Cry1C *Bt* toxin was found to be more effective at pH below 5 [7]. Another requirement for vesicle permeabilization was a 50% negatively charged lipid content for the membranes, suggesting that a negative surface potential promoted pore formation, a condition that promoted also Cry1C *Bt* toxin insertion in liposomes [7]. In the absence of acidic phospholipids, which are mostly restricted to the inner leaflet of cell membranes, a negative surface potential can be provided by glycoproteins and glycolipids, which are indeed localized, in substantial amounts, at the outer surface of cell membranes. However, if the proteins are internalized into cells, as has been suggested for the Bin toxin of *B. sphaericus* [18, 20, 44], they would encounter negative lipids on the internal compartments. Specificity for acidic lipids is typical of internalized toxins like diphtheria toxin [25, 30], *Pseudomonas* exotoxin A [26, 39] and clostridial neurotoxins [29].

Planar-lipid experiments provided direct evidence for the formation of ion channels by *Bs* toxins, although it cannot be totally excluded that other detergent effects of the proteins may have caused membrane destabilization. The PLB experiments were conducted in neutral phospholipids under experimental conditions (lipid composition and surface charge) that differed from those used in the LUV experiments, essentially because with vesicles, due to their small size and intrinsic low sensitivity, the optimum working conditions required the presence of at least 50% of negative lipids in the membrane. With PLBs instead, a neutral lipid composition was chosen because membranes were unstable with the lipid mixtures used for LUVs. Furthermore, neutral bilayers constitute the best environment to characterize the electrical properties of the pores by avoiding the presence of a negative surface potential.

As both vesicles and planar lipid bilayers are missing the *Bs* Bin toxin receptors that are present in *Bs*-sensitive mosquito cells [10, 11, 15, 51], it is quite possible that under our experimental conditions the insertion and assembly of the pores might have been an unfavorable event occurring only with a low frequency, similar to what was reported with *Bt* toxins [27, 33, 36, 46, 53] where reconstitution of the receptor in the bilayer resulted in significant increase in pore-formation efficacy [48]. On the other hand, a simple explanation for the rather high doses needed to observe permeabilization in LUVs, compared to PLBs, is the fact that forming a single channel in a PLB 250 μm in diameter requires a far smaller toxin concentration than forming a single pore in a vesicle 100 nm in diameter. Only a few pores are needed to observe single-channel activity in a bilayer area of 5×10^4 μm^2 (Fig. 5), whereas at least one pore per 0.1 μm^2 of vesicle membrane area is necessary to produce 30% of calcein release from LUVs (Fig. 2). In any case, the PLB technique is far more sensitive than the vesicle permeabilization technique, as it can detect the presence of one single channel located in the membrane and directly measure its biophysical properties, with the limitation that only the movement of charged entities can be measured.

Trypsin-activated Bin toxin inserted better in PLBs than the non-activated toxin and the channels formed were more stable and better resolved, consistent with the fact that activation increases the effect of Bin toxin on sensitive cells [1, 4, 10, 17]. However, activation actually reduced (or even suppressed) the ability of the toxin to permeabilize lipid vesicles. The activation process removes small peptides from the N- and C-termini of both components of Bin toxins [4]. This step may be required for high-affinity interaction of the toxins with their cellular receptor. It may not be absolutely needed

for insertion into neutral membranes, as observed in PLBs, whereas the presence of negatively charged lipids may be detrimental to activated toxin insertion into vesicles.

Because the Bin toxin is made of two structurally distinct components, it was interesting to investigate the role of each component and of their mixture using separately expressed and purified BinA and BinB proteins. To compare the reconstituted pair with the non-activated Bin toxin, the two recombinant components were added together (1:1, w/w) in the LUV experiments or PLB studies. In the case of LUVs, the mode of action of the Bin toxin and its reconstituted pair was quite similar (*compare* Figs. 2 and 4), although some clear differences could be detected. Firstly, the optimum pH was around 8.5 for the reconstituted pair instead of 10.5 with the Bin toxin. Secondly, the dose dependence was definitely more cooperative with the mixture of the two components, as indicated by the sigmoidal shape of the dose-effect curves and by the initial delay in the time course of permeabilization, neither of which was observed with the Bin toxin. Finally, the reconstituted pair permeabilized more than 90% of vesicles under optimal conditions (Fig. 3 and 4), whereas fewer than 40% of the vesicles were permeabilized by the full Bin toxin (Fig. 2). The reasons for these differences are not fully understood. Apparently, they are not due to the fact that in the Bin toxin, BinB is present in a slightly larger amount than BinA, as judged by SDS-PAGE (*not shown*). In fact, even when the recombinant BinB was twice as concentrated as the recombinant BinA (Fig. 3*A*), the dose dependence remained markedly sigmoidal. One difference that might be relevant is that while the recombinant BinB component is full-length, the recombinant BinA component is not, since 8 residues are missing from its N-terminus [44]. BinA is thus pseudo-activated even in the absence of trypsin treatment. While other studies have shown that 17 residues can be deleted at the N-terminus of BinA without loss of toxicity [44], it cannot be excluded that such deletion may affect some important steps involved in toxin-membrane interaction in vitro. In PLBs, both the non-activated and the activated Bin toxins induced channel activity. The activated toxin was more efficient and formed channels that were generally similar to those made by the BinA component alone. When the two recombinant components were mixed together in the PLB chambers and a new membrane was exposed to the mixture, BinA-like activity was observed, suggesting that the dominant channel former was BinA, consistent with the BinA signature of the activated, full Bin toxin.

When the activity of the single components and the effects of the order of addition were taken into account (Fig. 3, 6 and 7), some new concepts emerged: firstly, BinA alone was able to permeabilize the vesicles, but longer times and larger concentrations were needed in the absence of BinB. In PLBs, BinA alone made relatively stable, large channels; secondly, while BinB alone could not substantially permeabilize the vesicles, it improved the effect of BinA. However, BinB alone was able to form ion channels in PLBs, but the pores were much smaller and less stable than those made by BinA; thirdly, the presence of BinB enhanced the permeabilizing effect of BinA on LUVs and the channels made by BinB in PLBs adopted the BinA channel signature when BinA was also present in the bath; and finally, the amount of calcein release observed in the steady state depended mainly on the concentration of BinA, whereas the amount of BinB required to reach a given release was inversely related to that of BinA. This was also confirmed by the fact that BinB did not show any cooperativity, or synergism, with the full non-activated Bin toxin (*not shown*). Obviously, the amount of BinB component present in the original mixture was already high enough to express the full activity of the binary pair.

The mode of action of the toxin in artificial lipid membranes may therefore be explained by the fact that BinA is the component of the *Bs* Bin toxin, which displays the best pore-forming ability, whereas BinB actually assists and facilitates the formation of pores by BinA. This is in agreement with studies of BinB- and BinA-binding to brush border membranes prepared from the gut of *Culex pipiens* larvae, which showed that BinB promoted the specific binding of BinA [11, 44]. Furthermore, BinA at sufficiently high concentration, but not BinB, is toxic to *Culex pipiens* larvae [5, 23, 42] while BinA requires the presence of BinB to express its full activity [6]. Since with LUVs the largest effect, at least in terms of permeabilization rate (*see* Fig. 3C), was observed when BinB was already present at the addition of BinA, it is conceivable that BinB assists BinA at the earliest steps of pore formation, i.e., at the insertion stage of the protein into the membrane. The observation that both BinA and BinB can form pores, though with quite different efficiencies, is consistent with the fact that both proteins possess two homologous hydrophobic regions which could be involved in membrane insertion and pore formation [2].

This study suggests therefore that two main mechanisms are involved in pore formation by *Bs* Bin toxins, i.e., aggregation of and synergy between its two structural components. Such mechanisms have been proposed previously [13, 19, 49, 50]. Future work will involve characterizing the possible role of a receptor on pore formation by the individual components of the toxin and investigating their synergy using the PLB system, which appears to be particularly suitable to this aim, as demonstrated with the Cry1 Ac *Bt* toxin reconstituted in PLBs together with the *Manduca sexta* (tobacco hornworm, Lepidoptera) aminopeptidase-N receptor [48]. Also important will be to relate the observed pore-

forming properties with the BinB crystal structure, which is currently under elucidation [12].

This work was supported by the Royal Society (UK), the Italian Consiglio Nazionale delle Ricerche, by a grant from the Italian Istituto Trentino di Cultura to IB, by the French Institut Pasteur and by the National Research Council of Canada. NRCC No.: 44599

References

1. Baumann, L., Baumann, P. 1991. Effects of components of the *Bacillus sphaericus* toxin on mosquito larvae and mosquito-derived tissue culture-grown cells. *Curr. Microbiol.* **23:**51–57
2. Baumann, P., Clark, M.A., Baumann, L., Broadwell, A.H. 1991. *Bacillus sphaericus* as a mosquito pathogen: properties of the organism and its toxins. *Microbiol. Rev.* **55:**425–436
3. Bradford, M.M. 1976. A rapid and sensitive method for the quantitation of microgram quantities of protein utilizing the principle of protein-dye binding. *Anal. Biochem.* **72:**248–254
4. Broadwell, A.H., Baumann, P. 1987. Proteolysis in the gut of mosquito larvae results in further activation of the *Bacillus sphaericus* toxin. *Appl. Environ. Microbiol.* **53:**1333–1337
5. Broadwell, A.H., Baumann, L., Baumann, P. 1990. Larvicidal properties of the 42 and 51 kilodalton *Bacillus sphaericus* proteins expressed in different bacterial hosts: evidence for a binary toxin. *Curr. Microbiol.* **21:**361–366
6. Broadwell, A.H., Clark, M.A., Baumann, L., Baumann, P. 1990. Construction by site-directed mutagenesis of a 39-kilodalton mosquitocidal protein similar to the larva-processed toxin of *Bacillus sphaericus* 2362. *J. Bacteriol.* **172:**4032–4036
7. Butko, P., Cournoyer, M., Pusztai-Carey, M., Surewicz, W.K. 1994. Membrane interactions and surface hydrophobicity of *Bacillus thuringiensis* δ-endotoxin CryIC. *FEBS Lett.* **340:**89–92
8. Cevc, G. 1990. Membrane electrostatics. *Biochim. Biophys. Acta* **1031:**311–382
9. Charles, J.-F. 1987. Ultrastructural midgut events in Culicidae larvae fed with *Bacillus sphaericus* 2297 spore/crystal complex. *Ann. Inst. Pasteur/Microbiol.* **138:**471–484
10. Charles, J.-F., Nielsen-LeRoux, C., Delécluse, A. 1996. *Bacillus sphaericus* toxins: molecular biology and mode of action. *Annu. Rev. Entomol.* **41:**451–472
11. Charles, J.-F., Silva-Filha, M.H., Nielsen-LeRoux, C., Humphreys, M.J., Berry, C. 1997. Binding of the 51- and 42-kDa individual components from the *Bacillus sphaericus* crystal toxin to mosquito larval midgut membranes from *Culex* and *Anopheles* sp. (Diptera: Culicidae). *FEMS Microbiol. Lett.* **156:**153–159
12. Chiou, C.K., Davidson, E.W., Thanabalu, T., Porter, A.G., Allen, J.P. 1999. Crystallization and preliminary X-ray diffraction studies of the 51 kDa protein of the mosquito-larvicidal binary toxin from *Bacillus sphaericus*. *Acta Crystallogr.* **D55:**1083–1085
13. Cokmus, C., Davidson, E.W., Cooper, K. 1997. Electrophysiological effects of *Bacillus sphaericus* binary toxin on cultured mosquito cells. *J. Invertebr. Pathol.* **69:**197–204
14. Dadd, R.H. 1975. Alkalinity within the midgut of mosquito larvae with alkaline-active digestive enzymes. *J. Insect Physiol.* **21:**1847–1853
15. Darboux, I., Nielsen-LeRoux, C., Charles, J.-F., Pauron, D. 2001. The receptor of *Bacillus sphaericus* binary toxin in *Culex pipiens* (Diptera: Culicidae) midgut: molecular cloning and expression. *Insect Biochem. Mol. Biol.* **31:**981–990
16. Davidson, E.W. 1981. A review of the pathology of bacilli infecting mosquitoes, including an ultrastructural study of larvae fed *Bacillus sphaericus* 1593 spores. *Dev. Industr. Microbiol.* **22:**69–81
17. Davidson, E.W. 1986. Effects of *Bacillus sphaericus* 1593 and 2362 spore/crystal toxin on cultured mosquito cells. *J. Invertebr. Pathol.* **47:**21–31
18. Davidson, E.W. 1989. Variation in binding of *Bacillus sphaericus* toxin and wheat germ agglutinin to larval midgut cells of six species of mosquitoes. *J. Invertebr. Pathol.* **53:**251–259
19. Davidson, E.W., Oei, C., Meyer, M., Bieber, A.L., Hindley, J., Berry, C. 1990. Interaction of the *Bacillus sphaericus* mosquito larvicidal proteins. *Can. J. Microbiol.* **36:**870–878
20. Davidson, E.W., Schellabarger, C., Meyer, M., Bieber, A.L. 1987. Binding of the *Bacillus sphaericus* mosquito larvicidal toxin to cultured insect cells. *Can. J. Microbiol.* **33:**982–989
21. Davidson, E.W., Titus, M. 1987. Ultrastructural effects of the *Bacillus sphaericus* mosquito larvicidal toxin on cultured mosquito cells. *J. Invertebr. Pathol.* **50:**213–220
22. de Barjac, H., Lecadet, M.-M. 1976. Dosage biochimique de l'exotoxine thermostable de *B. thuringiensis* d'après l'inhibition d'ARN-polymérases bactériennes. *C.R. Acad. Sc. Paris* **282:**2119–2122
23. De la Torre, F., Bennardo, T., Sebo, P., Szulmajster, J. 1989. On the respective roles of the two proteins encoded by the *Bacillus sphaericus* 1593M toxin genes expressed in *Escherichia coli* and *Bacillus subtilis*. *Biochem. Biophys. Res. Comm.* **164:**1417–1422
24. English, L., Slatin, S. 1992. Mode of action of delta-endotoxins from *Bacillus thuringiensis*: a comparison with other bacterial toxins. *Insect Biochem. Molec. Biol.* **22:**1–7
25. Eriksen, S., Olsnes, S., Sandvig, K., Sand, O. 1994. Diphtheria toxin at low pH depolarizes the membrane, increases the membrane conductance and induces a new type of ion channel in Vero cells. *EMBO J.* **13:**4433–4439
26. Gambale, F., Rauch, G., Belmonte, G., Menestrina, G. 1992. Properties of *Pseudomonas aeruginosa* exotoxin A ionic channel incorporated in planar lipid bilayers. *FEBS Lett.* **306:**41–45
27. Grochulski, P., Masson, L., Borisova, S., Pusztai-Carey, M., Schwartz, J.L., Brousseau, R., Cygler, M. 1995. *Bacillus thuringiensis* CryIA(a) insecticidal toxin: crystal structure and channel formation. *J. Mol. Biol.* **254:**447–464
28. Harvey, A.L. 1990. Cytolytic toxins. *In:* Handbook of Toxinology. Shier, W.T., Mebs, D., editors. pp. 1–66. Marcel Dekker, New York
29. Herreros, J., Lalli, G., Montecucco, C., Schiavo, G. 1999. Pathophysiological properties of clostridial neurotoxins. *In:* The Comprehensive Sourcebook of Bacterial Protein Toxins. Alouf, J.E., Freer, J.H. editors. pp. 202–228. Academic Press, London
30. Jiang, G.-S., Solow, R., Hu, V.W. 1989. Characterization of diphtheria toxin-induced lesions in liposomal membranes. *J. Biol. Chem.* **264:**13424–13429
31. Kagawa, Y., Racker, E. 1971. Partial resolution of the enzymes catalyzing oxidative phosphorylation. XXV. Reconstitution of vesicles catalyzing inorganic phosphorus-32-adenosine triphosphate exchange. *J. Biol. Chem.* **246:**5477–5487
32. Kayalar, C., Duzgunes, N. 1986. Membrane action of colicin E1: detection by the release of carboxyfluorescein and calcein from liposomes. *Biochim. Biophys. Acta* **860:**51–56
33. Knowles, B.H., Blatt, M.R., Tester, M., Horsnell, J.M., Carroll, J., Menestrina, G., Ellar, D.J. 1989. A cytolytic δ-endotoxin from *Bacillus thuringiensis* var. *israelensis* forms cation selective channels in planar lipid bilayers. *FEBS Lett.* **244:**259–262
34. Lacy, D.B., Stevens, R.C. 1998. Unraveling the structures and

modes of action of bacterial toxins. *Curr. Opin. Struct. Biol.* **8:**778–784

35. Lesieur, C., Vécsey-Semjén, B., Abrami, L., Fivaz, M., van der Goot, F.G. 1997. Membrane insertion: the strategies of toxins. *Mol. Membrane Biol.* **14:**45–64
36. Lorence, A., Darszon, A., Díaz, C., Liévano, A., Quintero, R., Bravo, A. 1995. δ-Endotoxins induce cation channels in *Spodoptera frugiperda* brush border membranes in suspension and in planar lipid bilayers. *FEBS Lett.* **360:**217–222
37. MacDonald, R.C., MacDonald, R.I., Menco, B.P.M., Takeshita, K., Subbarao, N.K., Hu, L. 1991. Small-volume extrusion apparatus for preparation of large, unilamellar vesicles. *Biochim. Biophys. Acta* **1061:**297–303
38. Manivannan, K., Ramanan, S.V., Mathias, R.T., Brink, P.R. 1992. Multichannel recordings from membranes which contain gap junction. *Biophys. J.* **61:**216–227
39. Menestrina, G., Pederzolli, C., Forti, S., Gambale, F. 1991. Lipid interaction of *Pseudomonas aeruginosa* exotoxin A: acid triggered aggregation and permeabilization of lipid vesicles. *Biophys. J.* **60:**1388–1400
40. Menestrina, G., Vécsey-Semjén, B. 1999. Biophysical methods and model membranes for the study of bacterial pore-forming toxins. *In:* The Comprehensive Sourcebook of Bacterial Protein Toxins. Alouf, J.E., Freer, J.H. editors. pp. 287–309. Academic Press, London
41. Müller, P., Rudin, D.O., Tein, H.T., Wescott, W.C. 1963. Methods for formation of single bimolecular lipid membranes in aqueous solution. *J. Phys. Chem.* **67:**534–535
42. Nicolas, L., Nielsen-LeRoux, C., Charles, J.-F., Delécluse, A. 1993. Respective role of the 42- and 51-kDa components of the *Bacillus sphaericus* toxin overexpressed in *Bacillus thuringiensis*. *FEMS Microbiol. Lett.* **106:**275–280
43. Nielsen-LeRoux, C., Charles, J.-F. 1992. Binding of *Bacillus sphaericus* binary toxin to a specific receptor on midgut brush-border membranes from mosquito larvae. *Eur. J. Biochem.* **210:**585–590
44. Oei, C., Hindley, J., Berry, C. 1992. Binding of purified *Bacillus sphaericus* binary toxin and its deletion derivatives to *Culex quinquefasciatus* gut: elucidation of functional binding domains. *J. Gen. Microbiol.* **138:**1515–1526
45. Schnepf, E., Crickmore, N., Van Rie, J., Lereclus, D., Baum, J., Feitelson, J., Zeigler, D.R., Dean, D.H. 1998. *Bacillus thuringiensis* and its pesticidal crystal proteins. *Microbiol. Mol. Biol. Rev.* **62:**775–806
46. Schwartz, J.-L., Garneau, L., Savaria, D., Masson, L., Brousseau, R., Rousseau, E. 1993. Lepidopteran-specific crystal toxins from *Bacillus thuringiensis* form cation- and anion-selective channels in planar lipid membranes. *J. Membrane Biol.* **132:**53–62
47. Schwartz, J.L., Laprade, R. 2000. *Bacillus thuringiensis* toxins: membrane permeabilization and pore formation. *In:* Entomopathogenic Bacteria: from Laboratory to Field Application. Charles, J.-F., Delécluse, A., Nielsen-LeRoux, C. editors. pp. 199–218. Kluwer Associate Publishing, Norwell, MA
48. Schwartz, J.-L., Lu, Y.J., Söhnlein, P., Brousseau, R., Laprade, R., Masson, L., Adang, M.J. 1997. Ion channels formed in planar lipid bilayers by *Bacillus thuringiensis* toxins in the presence of *Manduca sexta* midgut receptors. *FEBS Lett.* **412:**270–276
49. Sgarella, F., Szulmajster, J. 1987. Purification and characterization of the larvicidal toxin of *Bacillus sphaericus* 1593M. *Biochem. Biophys. Res. Commun.* **143:**901–907
50. Shanmugavelu, M., Rajamohan, F., Kathirvel, M., Elangovan, G., Dean, D.H., Jayaraman, K. 1998. Functional complementation of nontoxic mutant binary toxins of *Bacillus sphaericus* 1593M generated by site-directed mutagenesis. *Appl. Environ. Microbiol.* **64:**756–759
51. Silva-Filha, M.H., Nielsen-LeRoux, C., Charles, J.-F. 1997. Binding kinetics of *Bacillus sphaericus* binary toxin to midgut brush-border membranes of *Anopheles* and *Culex* sp. mosquito larvae. *Eur. J. Biochem.* **247:**754–761
52. Silva-Filha, M.H., Nielsen-LeRoux, C., Charles, J.-F. 1999. Identification of the receptor for *Bacillus sphaericus* crystal toxin in the brush border membrane of the mosquito *Culex pipiens* (Diptera: Culicidae). *Insect Biochem. Mol. Biol.* **29:**711–721
53. Slatin, S.L., Abrams, C.K., English, L. 1990. Delta-endotoxins form cation-selective channels in planar lipid bilayers. *Biochem. Biophys. Res. Commun.* **169:**765–772
54. Tejuca, M., Dalla Serra, M., Ferreras, M., Lanio, M.E., Menestrina, G. 1996. The mechanism of membrane permeabilization by sticholysin I, a cytolysin isolated from the venom of the sea anemone *Stichodactyla helianthus*. *Biochemistry* **35:**14947–14957
55. Yoshida, N., Tamura, M., Kinjo, M. 2000. Fluorescence correlation spectroscopy: a new tool for probing the microenvironment of the internal space of organelles. *Single Mol.* **1:**279–283